J Mater Sci: Mater Med (2011) 22:1555–1567
DOI 10.1007/s10856-011-4316-5

Fabrication of nano-structured electrospun collagen scaffold intended for nerve tissue engineering

A. Timnak · F. Yousefi Gharebaghi · R. Pajoum Shariati · S. H. Bahrami · S. Javadian · Sh. Hojjati Emami · M. A. Shokrgozar

Received: 28 November 2010 / Accepted: 4 April 2011 / Published online: 28 April 2011

Abstract Nerve tissue engineering is one of the most promising methods in nerve tissue regeneration. The development of blended collagen and glycosaminoglycan scaffolds can potentially be used in many soft tissue engineering applications. In this study an attempt was made to develop two types of random and aligned electrospun, nanofibrous scaffold using collagen and a common type of glycosaminoglycan. Ion chromatography test, MTT and attachment assays were conducted respectively to trace the release of glycosaminoglycan, and to investigate the biocompatibility of the scaffold. Cell cultural tests showed that the scaffold acted as a positive factor to support connective tissue cell outgrowth. The positive effect of fiber orientation on cell outgrowth organization was traced through SEM images. Porosity percentage calculation and tensile strength measurement of the webs specified analogous properties to the native neural matrix tissue. These results suggested that nanostructured porous collagen-glycosaminoglycan scaffold is a potential cell carrier in nerve tissue engineering.

A. Timnak · F. Yousefi Gharebaghi · Sh. Hojjati Emami
Faculty of Biomedical Engineering, Amirkabir University of Technology, 424 Hafez Ave, 15875-4413 Tehran, Iran

R. Pajoum Shariati
Faculty of Chemical Engineering, Amirkabir University of Technology, 424 Hafez Ave, 15875-4413 Tehran, Iran

S. H. Bahrami
Faculty of Textile Engineering, Amirkabir University of Technology, 424 Hafez Ave, 15875-4413 Tehran, Iran

S. Javadian
Department of Biochemistry, Pasteur Institute of Iran, 13169-43551 Tehran, Iran

M. A. Shokrgozar (✉)
National Cell Bank of Iran, Pasteur Institute of Iran, 13169-43551 Tehran, Iran
e-mail: mashokrgozar@pasteur.ac.ir

1 Introduction

Tissue engineering is a technique in biomedical engineering to repair, replace or maintain the function of defective or damaged tissues or organs [1].

It is well known that the nervous tissue defects are among those defects which could not be repaired spontaneously. Traditionally, tissue transplantation or peripheral nerve grafting were used to repair damaged or diseased region of the nervous system, but this procedure often encountered donor shortage and immunological problems associated with infectious disease. Recently, tissue engineering has provided a new medical therapy as an alternative to conventional transplantation methods based on the use of biomaterials with or without living precursor cells. Cells live in a complex mixture of pores, ridges and fibers of ECM at nanometer scales. Hence, a nano-structured porous scaffold with pores and large surface area is needed as an alternative to natural ECM for better cell ingrowth in a three dimensional fashion. As per literature survey, several methods have been reported to fabricate polymeric nanofibers or submicrofibers by using phase separation, electrospinning, and self assembly [1].

The key point in the success of a tissue engineering technique is to mimic the structural and functional properties of a native tissue. Extracellular matrix (ECM) is the basement membrane of cells in the biological environment of the body. The more the designed scaffold resembles the native tissue, the more efficient the cell-scaffold interaction would be. As it is known, ECM is mainly composed of

Collagen, frequently with a fibrous-like structure and various nano-sized diameters. Among all the techniques which are used in synthesizing the scaffolds, electrospinning is the most well-known in nanofiber production [2–4].

The collagen fibril provides the key to scaffolding structures in the body [2, 5]. Glycosaminoglycans (GAGs) are glycoproteins with a protein core and polysaccharide branches. Collagen and GAG are widely utilized to fabricate scaffolds, serving as an active analog of native ECM. Both of them have been found to enhance biological interactions with cells and speed up tissue regeneration [2–4].

Traditional collagen–GAG scaffolds in gel or sponge form have been extensively manufactured. However, these scaffolds exhibit poor mechanical properties and unacceptable physical structure for many specific organ or tissue regeneration. This is due to the great differences existing between native ECM and manufactured scaffolds [3, 4].

Electrospinning is a process that utilizes a strong electrostatic field to obtain ultrafine fibers from a polymer solution or molten medium [6, 7]. Most of the nanofibers produced by electrospinning are collected into a nonwoven web form, which generally gives random fiber orientation and poor mechanical properties. Most native ECMs found in tissues or organs, however, have regular or defined orientation architecture, which is significant for tissue function [2–4].

As cell orientation and its cytoskeleton organization define cell function, it is expected that the use of specifically oriented fibers would lead to closer simulation of body environment [8, 9].

In this study we made an attempt to fabricate a biodegradable nanofibrous porous scaffold by Electrospinning method, using collagen and GAG with a structure similar to natural ECM to support cell outgrowth in vitro.

2 Materials and methods

2.1 Materials

Main chemicals and reagents used in this study included calf skin type I collagen extracted in the Cell Bank department of Pasteur institute of Iran, chondroitin-6-sulfate (C6S) (Sigma Aldrich Chemical Co), 1,1,1,3,3,3 hexafluoro-2-propanol (HFP) (Sigma Aldrich Chemical Co), genipin (Wako Chemicals GmbH, Japan), 3-(4,5-dimethylazol-2-yl)-2,5-diphenyl-2H-tetrazolium bromide (MTT), Dulbecco's modified Eagle's medium (DMEM) (Gibco), and fetal bovine serum (FBS) (Hyclone), Trypsin + EDTA, PBS.

2.2 Methods

2.2.1 Preparation of nanofibrous collagen scaffold

In this research, HFP the ordinary solvent of proteins, was used as a component of the solvent. A 7% w/v solution of Collagen in the relevant solvent of 1,1,1,3,3,3-hexafluoro-2-propanol (HFP):Acetic Acid (AAc) (1:1) was used as the optimum electrospinning solution in order to achieve the ideal nanofibrous scaffold.

2.2.2 Preparation of nanofibrous collagen/chondroitin sulfate composite scaffold

In order to get the composite scaffold, a solution with the collagen/Chondroitin Sulfate (CS, a common GAG) with the ratio of 98/2 was prepared. After this solution had been kept in the refrigerator for 24 h, it was sent for electrospinning process.

2.2.3 Optimizing the electrospinning process parameters

During electrospinning, the solution was placed into a 10 ml syringe fitted to an 18 gauge needle. Three parameters including Voltage, Feed Rate and nozzle to target distance which were of much more significance among the other parameters were optimized. A syringe pump was used to feed the solution into the needle tip at a feed rate of 0.2–0.7 ml/h. A voltage of 10–20 kV provided by a high voltage power source was applied between the needle (anode) and the grounded collector (cathode) with the distance of 13–20 cm. Finally, the optimized group was set at, vol. of 15 kV, feed rate of 0.2 ml/h and the needle to collector distance of 20 cm.

2.2.4 Oriented collection of the fibers

As the orientation of the fibers in electrospun scaffolds directly affects the cellular organization and orientation, in order to get an aligned fibrous scaffold we used a cylindrical collector (GOLDSTAR FZ-180) with an adjustable speed at three rates of 2600, 3400 and 5000 rpm. Rotating speed of the collector directly affects both size (diameter) and morphology of the webs. Investigation of the results pointed to the optimum speed of 2600 rpm. The process is schematically shown in Fig. 1.

2.2.5 Crosslinking of the scaffolds

The traditional method in crosslinking of the protein-based electrospun scaffolds is Glutaraldehyde (GA) vapor exposure. But, recently, Genipin (GP) has been reported as a crosslinking agent of cellular and acellular tissues, as well

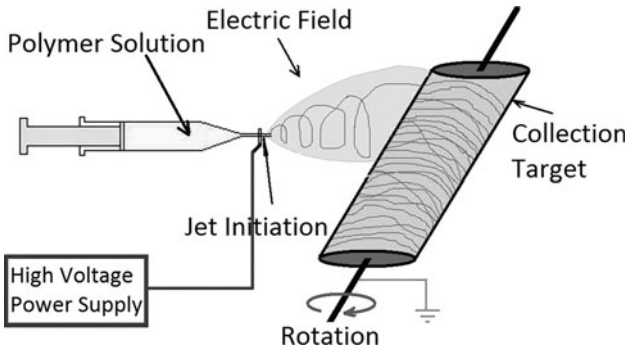

Fig. 1 Schematic of electrospinning setup and process with cylindrical collector to get aligned fibers

Table 1 Four groups of crosslinking solution concentration-crosslinking time combination

	Grp. 1	Grp. 2	Grp. 3	Grp. 4
Genipin solution concentration (mM)	3.5	3.5	5	5
Crosslinking duration (days)	3	5	3	5

as biomaterials. Genipin is a novel kind of natural crosslinker whose cytotoxicity is 5,000 to 10,000 times lower than GA [10–15].

Collagen is white in crystalline form and produces a clear solution when dissolved in water or saline. Collagen crosslinking with genipin has two unique outcomes: (1) following crosslinking with genipin, normally opaque collagen turns blue, and (2) these crosslinks emit fluorescence at 630 nm when excited at 590 nm [16, 17].

In this research the electrospun collagen-based scaffolds were soaked in two 5 and 3.5 mM aqueous genipin solutions and each for two periods of 3 and 5 days. In short, four groups (grp.) as is shown in Table 1, were adjusted for further cytotoxicity evaluation.

Specimens of 1.5 cm × 2 cm were cut out of the mats. Then each of them was crosslinked with the four distinctive crosslinking solutions. Next each specimen was soaked in 1 ml of the proper crosslinking solution and incubated either 3 or 5 days in centrifuge tubes at 37°C.

After crosslinking, the scaffolds were rinsed three times in 1% PBS solution for 15 min to quench unreacted GP.

The first outcome of collagen crosslinking, turning the opaque appearance of collagen to blue, was obviously observed with naked eye. And the second outcome, emission of red fluorescence as a consequence of exciting at the proper wavelength, was probed by Fluorescence microscope.

2.2.6 *Scanning electron microscopy*

Fiber morphology of the non-crosslinked and crosslinked scaffolds was visualized and compared by use of a scanning electron microscope (XL30 Philips). The SEM scanning was performed at an accelerating voltage of 25 kV. The diameters of the fibers were measured from SEM images with an image analysis program (Motic Images Plus 2.0).

2.2.7 *Physical and mechanical evaluation of the scaffolds*

Uniaxial material testing was performed in dry state and on a mechanical testing system (Siber Tensile Tester, Fafegraph M, Textechno) incorporating a 10 N load cell with an extension rate of 0.16 mm/s to failure. Five (n = 5) test specimens were tested in each of the following orientations (random and regular oriented fibers). The specimens were cut out of the mats (15 mm × 3 mm) [14, 18] and ranged in thickness from 0.01 to 0.07 mm. Since the tensile specimens were cut through different parts of the main mat, to minimize the effect of the difference in the porosity % in various parts of the mat from one tensile specimen to another, each specimen was cut in precise weight of 0.0013 g (equal weight–equal porosity). The material properties chosen for comparison were the peak stress, and the strain to failure (also calculated automatically by the tensile system).

Scaffold porosity was estimated using the following equation [7, 19]:

$$\text{Porosity} = \frac{(1-\rho_S)}{\rho_M} \times 100 \quad (1)$$

where ρ_S and ρ_M (=0.9667 g/cm^3) are the scaffold and material densities, respectively. This equation provides an accurate measurement of the porosity, with an estimated error of 2%, but cannot distinguish between open and closed porosity.

2.2.8 *Cell culture*

For sterilization, the scaffolds were soaked in 70% ethanol for 2 h. SK-N-MC human neuroblastoma cell lines (courtesy of Cell Bank department of Pasteur institute of Iran) and human normal Fibroblast extracted from bone tissue in the Tissue Engineering lab of Cell Bank department of Pasteur institute of Iran were routinely grown in Dulbecco's modified Eagle's medium (DMEM) containing 10% (vol/vol) fetal bovine serum (FBS) (DMEM-10% FBS). Cells were maintained at 37°C in a saturated humidity atmosphere incubator in 75 cm^2 flasks. For cell culture experiments, SK-N-MC and Fibroblast were detached by means of Trypsin/EDTA solution, resuspended in DMEM-10% FBS and seeded at a concentration of 5 × 10^5 cells/ml on (1 cm × 1 cm) samples of each of the 2 kinds of scaffolds produced, placed on the bottom of a 24-well cell culture plate. Cells were allowed to grow

in DMEM-10% FBS on different substrates for 7 days. At the end of the seventh day, cells were fixed on the scaffold surfaces for SEM observation.

2.2.9 MTT assay

MTT assay determines viable cell numbers and is based on the mitochondrial conversion of the tetrazolium salt, 3-[4,5-dimethylthiazol-2-yl]-2,5 diphenyltetrazolium bromide (MTT). Modified MTT assay was employed in this study to quantitatively assess the cytotoxicity of crosslinked Collagen/GAG scaffolds.

Each 3 cm^2 crosslinked specimen was incubated in 4 ml absolute DMEM in 37°C incubator for intervals of 3, 7 and 14 days. The control group (absolute culture medium) was also treated the same way. The media collected at days 3, 7 and 14 were kept in the refrigerator until use.

On the first day of testing, SK-N-MC and fibroblast were seeded on a 96-well culture plate with cell density of 2×10^4 cells/well in fresh DMEM-10% FBS and incubated for 24 h; the second day the medium was removed and reconstituted with the 3rd, 7th and 14th day extract of each group crosslinked scaffold + 10% FBS and incubated overnight. The medium was then totally removed and MTT reagent (100λ, 0.5 mg/ml) was added to each well of the 96-well plate and left to incubate for 4 h at 37°C. The MTT reagent was replaced with 100λ of isopropanol to dissolve the formazan crystals. The absorbance was measured at 570 nm using an ELISA plate reader (Stat fax-2100 USA).

2.2.10 Ion chromatography test

In order to determine the amount of GAG release and also to vindicate the MTT assay results, Ion (Sulfate) chromatography test was conducted. In this test, IC (Metrohm No. 761) with the following specification was used:

Ionic column: 6.1006.100 METROSEP Anion Dual 2, Eluent: 2 mmol/l $NaHCO_3$/1.3 mmol/l Na_2CO_3 (with chemical suppression), Loop: 20 µl and Flow: 0.8 ml/min.

Calibration of the system was conducted with 3 standard points of 1, 5 and 10 ppm with Fluka 89886.

Twelve ml of samples from each of the four crosslinking groups were sent to the biochemistry laboratory for measuring the concentration of sulfate groups in the medium.

2.2.11 Cell attachment experiment

Cell attachment assays determine the fraction of cells that attach to matrix surfaces and are resistant to gentle washing [20].

The cell attachment experiments were conducted in a three stage test, on the 1st, 3rd and 7th day. The main purpose of the first day stage of the test was to investigate the attachment affinity of the cells to the surface of the scaffold, and in the 3rd and 7th day stage, the role of the scaffolds composition in cell proliferation was investigated and compared with the control sample.

The bottoms of 6 wells of a 24-well cell culture plate were totally covered with scaffold. The control samples were the bottom of cell culture plates. At the first stage, 2,000 cells were allowed to attach for 90 min in each well, before scaffolds/plates were washed gently with PBS and aspirated. Cell attachment was then assessed in 3 replicates using cell counting quantitative method, using trypsin solution and neubauer lam. In the second and third stages of the test, the washing step was omitted, and at the end of the 3rd and 7th day, the viability of cells was compared in test samples and controls.

2.2.12 Statistical analysis

All statistics are based on a Dunnet one way analysis of variance (ANOVA) on ranks. The a priori alpha value was set at 0.05 with significance defined as $P < 0.05$.

3 Results

3.1 Optimizing electrospinning process

3.1.1 Viscosity

In order to analyze the effect of solution viscosity on fiber diameter, electrospinning of four solutions with the concentrations of 18, 15, 10 and 7% w/v was conducted. It is deduced that by increasing the solution viscosity the diameter of the fibers also increase.

Favorable fiber diameter and scaffold application can be achieved by careful selection of solution viscosity. To attain the fibers with diameters in nano-scale the concentration of 7% w/v was selected.

Figure 2 shows the representative images of fibrous scaffolds for solutions with different amounts of viscosity.

3.1.2 Electric field strength

The effect of electric field strength was traced through the SEM micrographs. Three experiments were run with electric field strength of 20, 15 and 10 kV, while the other parameters were kept unchanged.

It can be inferred from Fig. 3a) that, the voltage of 10 kV was able to initiate the jet but not a smooth one. The voltage was increased to obtain a more homogenous web as shown in Fig. 3b). But further increasing in electric field strength caused the mat to be formed with more defects (Fig. 3c).

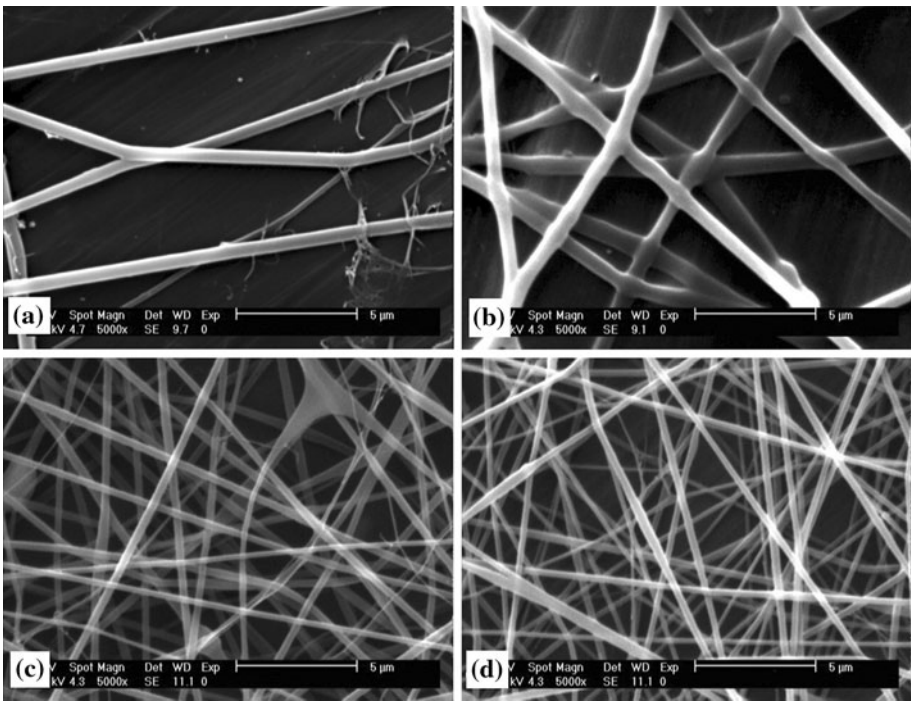

Fig. 2 Collagen electrospinning solution with collagen concentrations of **a** 18%, **b** 15%, **c** 10% and **d** 7% w/v in HFP:AAc solvent

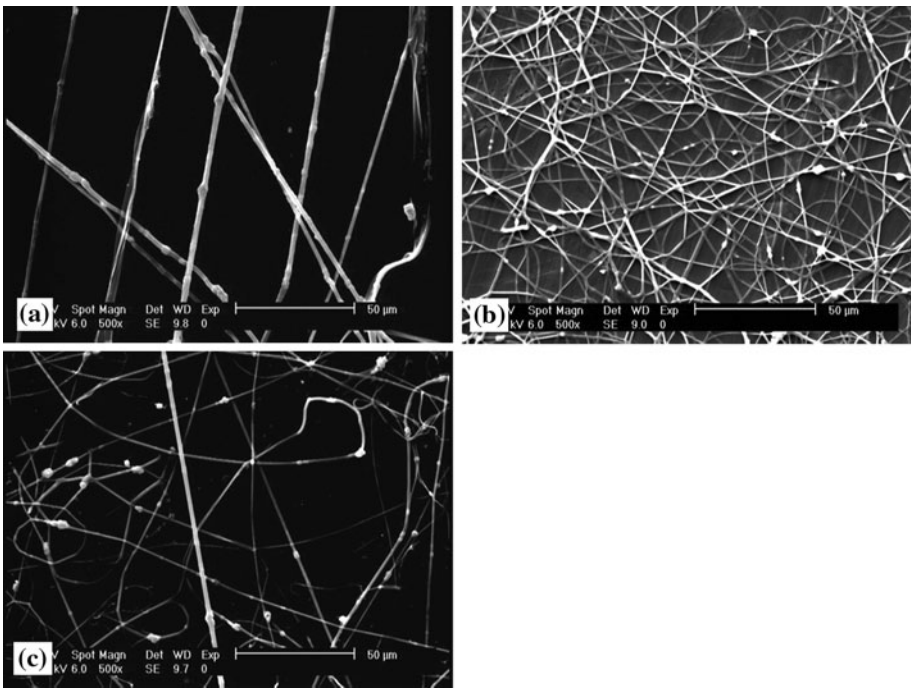

Fig. 3 The effect of voltage increase on the fibers morphology. **a** 10 kV, **b** 15 kV and **c** 20 kV. Other parameters are kept constant

Accordingly, it seems that there is no identified manner for optimizing this parameter and the "try and error" procedure must be followed.

3.1.3 Solution flow rate

Solution flow rate is one of the secondary factors which affect the fibers morphology. Solution flow rate and electric field strength are correlative parameters whose values fluctuate according to the change of the value in one or the other. Considering the value which was set for electric field strength, solution flow rate parameter was also adjusted. Keeping all parameters constant, three values of 0.2, 0.5 and 0.7 ml/h were set for solution flow rate. In Fig. 4, the effect of this parameter can be detected. Taking Fig. 4 into consideration supports the conclusion that the most

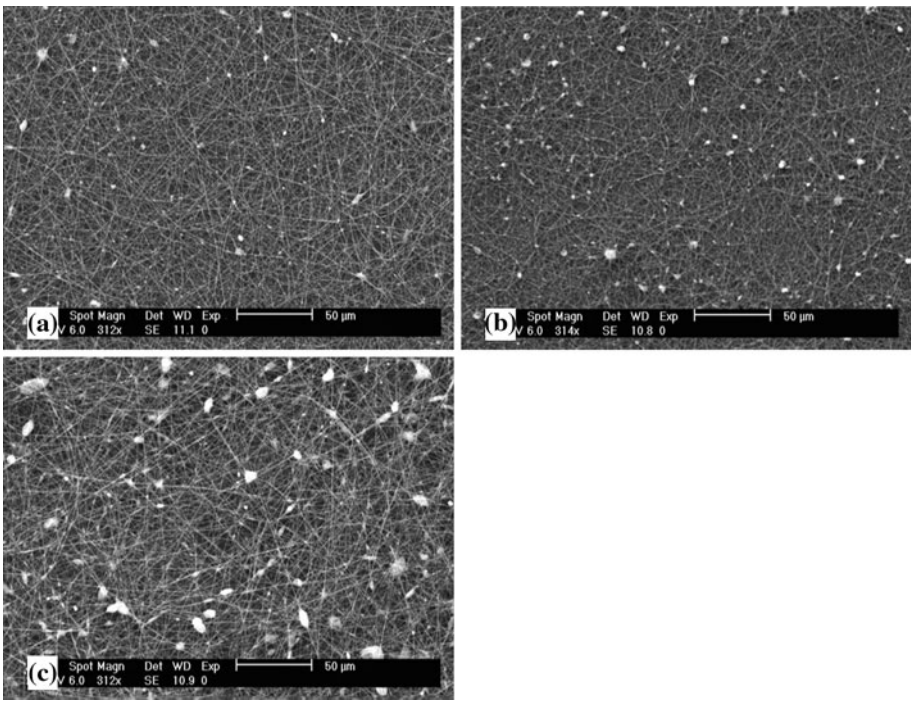

Fig. 4 Solution flow rate as a secondary factor affecting the fibers homogeneity. Flow rate and voltage conjugation is a factor that must be optimized according to the situation. As in the previous phase voltage was set on 15 kV so the proper amount of flow rate was decided in the current phase. **a** 0.2, **b** 0.5 and **c** 0.7 ml/h

efficient combination of solution flow rate and electric field strength is obtained at 0.2 ml/h and 15 kV respectively.

3.1.4 Nozzle to target distance

Nozzle to target distance is another factor affecting the morphology and homogeneity of the scaffold. This parameter is among the factors which have no specific effect on the fiber diameter (Chart 1). According to the experiments which were conducted in this phase, it can be inferred that during the period in which the electric filed is not interrupted, an increase in the Nozzle to target distance leads to a more homogenous structure. The effect of this parameter is shown in Figs. 5 and 6.

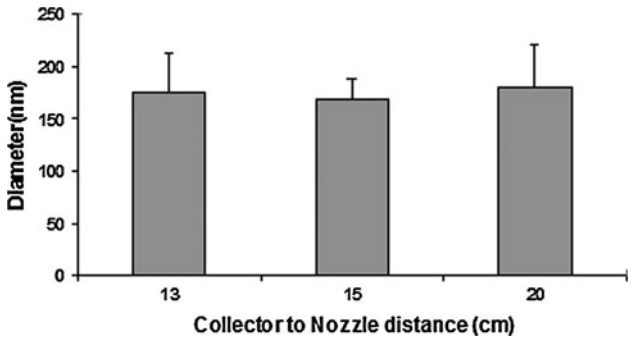

Chart 1 Changing nozzle to target distance has no specific effect on fibers mean diameter

3.2 Scaffold characterization

3.2.1 Tensile strength of intact nerves and extracted nerve scaffolds

Tensile strength of scaffold was measured and was compared with the properties of an intact nerve which was assessed [21] by the same test factors as the scaffolds. The results, summarized in Table 2, indicate that the strategy of orienting the fibers appears successful in improving the tensile property of the scaffold. As it is presented in Table 2 the ultimate strength of aligned scaffold in comparison with random fibrous scaffold is much closer in value to intact normal nerve. From a different viewpoint, ultimate strains of both the extracted scaffolds are higher in value compared to the normal nerve [21]. Discussing the data, it is obvious that the higher magnitude of ultimate stress in aligned fibrous scaffolds compared with random fibrous scaffolds, points to a stiffer structure of the aligned structure. Consequently, its relative ultimate strain is lower (compared to random fibrous scaffold).

As demonstrated by the statistical analysis of the data, oriented collecting of the fibers has a profound effect on improving the tensile strength of the scaffold.

3.2.2 Porosity percentage evaluation of scaffolds

Porosity and surface area are two important variables affecting interaction of structures with the host environment [7]. It is clear that as far as the porosity value of the

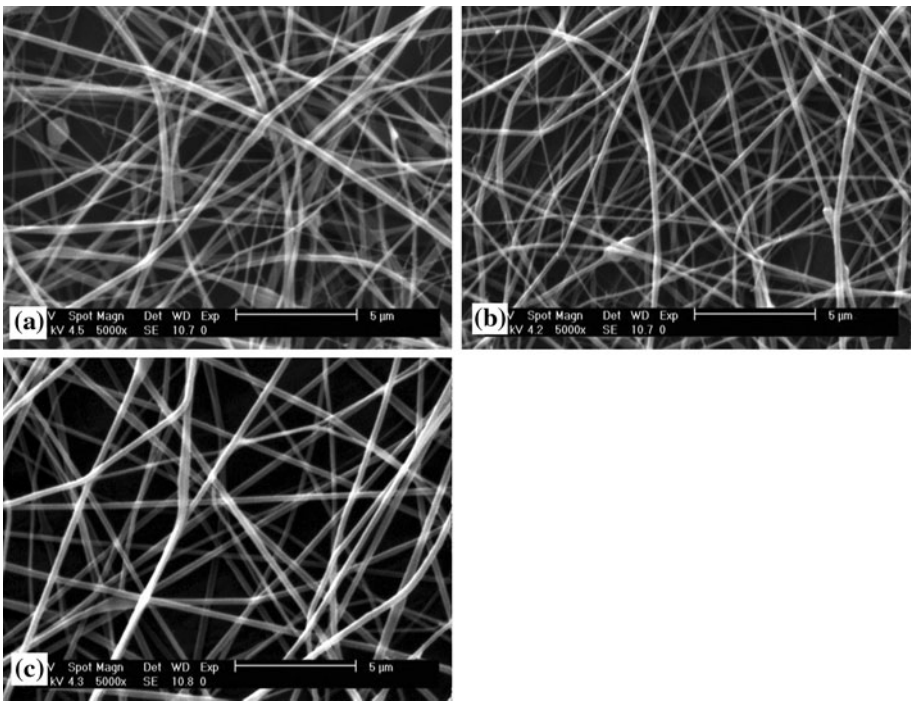

Fig. 5 Nozzle to target distance, a factor which affects the homogeneity of web structure, and no specific effect on fibers mean diameter. As is shown, increasing the distance have had positive effect on structure homogeneity, **a** 13 cm, **b** 15 cm and **c** 20 cm

membrane increases, the amount of surface area will increase accordingly. The porosity of randomly orientated electrospun collagen/GAG scaffolds was estimated at 80.68% using the equation.

3.2.3 Morphology of aligned nanofibrous scaffold

In order to get organized oriented fibrous webs, collection of the fibers was conducted at speeds of 2600, 3400 and 5000 rpm which refers to rotating speed of the collector. The overall outcome indicated that by increasing the collection speed from 2,600 to 5,000 rpm, the diameter of the fibers decrease, whereas homogeneity of the structure undergoes a reduction. As the defective and beaded structure affects cell outgrowth negatively, the speed rate of 2,600 rpm was selected. The morphological structure of electrospun nanofibrous collagen was observed by SEM. As shown in Fig. 7, though the alignment of every fiber is not perfect in the same orientation, a distinct regularity of the collagen fibers with a specific aligned longitudinal topography is shown on the aligned scaffold Fig. 7a. In comparison, the fibers on the random scaffold Fig. 7b exhibited a more random orientation.

3.3 In vitro cell culture study

Attachment and spreading of the SK-N-MC and fibroblast on the scaffold surface were both observed by SEM micrographs as shown in Figs. 8 and 9.

In the in vitro cell culture tests, we demonstrated the biocompatibility of the scaffolds to the cells and proved that the scaffold is very important in making the cellular morphology and the cells outgrowth.

In Figs. 8 and 9 the cells were shown to align parallel to the orientation of the Collagen nanofibers.

As mentioned earlier, most cell types adhere and elongate themselves along the alignment direction of the nanofibers. The comparison of the micrographs of cell organization on the random fibrous scaffold (data not shown) suggests that the fibers may regulate the cell orientation during proliferation. Proliferation of the two aforementioned cell types in the crosslinked collagen–GAG scaffolds' extract was analyzed by MTT assay. The results of this assay are presented in Chart 2.

MTT assay results revealed that as time passes, each group experiences a decrease in the value of the cell viability factor. In order to more precisely explain the MTT assay results, C6S release (mg/l) into the culture medium, was measured by chromatography technique and the results are shown in Fig. 10. In the chromatography test, the released amount of C6S was in direct relationship with the released amount of sulfate. Positive slope of the release profile in parts a and b of Fig. 10, points to ascending release of C6S. However, this release takes a descending pattern in parts c and d of Fig. 10 as time passes. Based on the slope of release profiles, it can be inferred that samples of the first and the second group possess better conditions than the samples of the third and the fourth group.

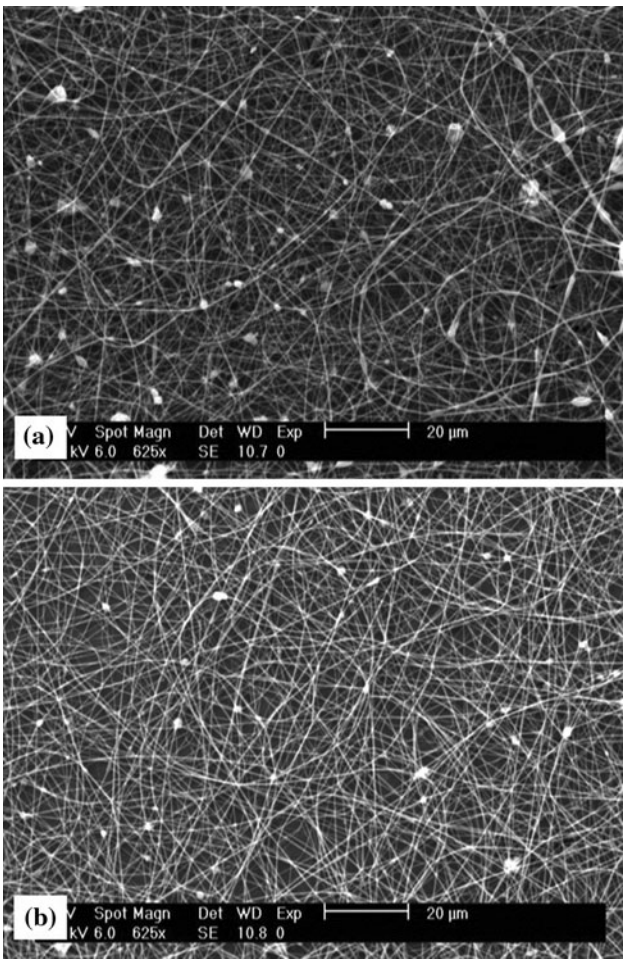

Fig. 6 Effect of nozzle to target distance parameter on web structure with a lower magnification index (with respect to Fig. 5). **a** 15 cm and **b** 20 cm

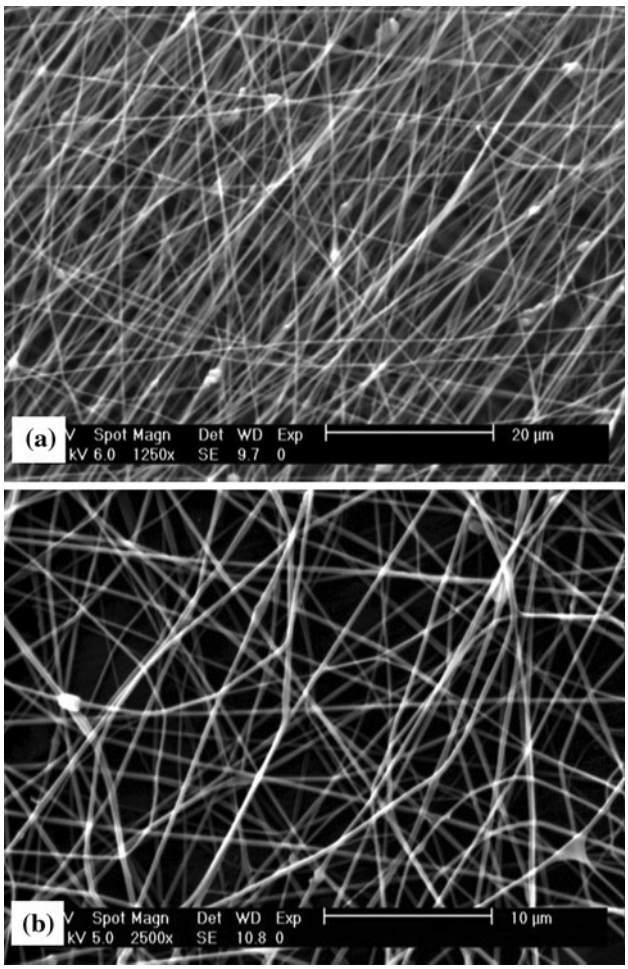

Fig. 7 Comparison of the morphological structure of two electrospun webs, collected in two different manners. **a** Regularity of the fibers with a specific aligned topography, collected with a cylindrical rotating collector, **b** random structure of web, collected on fixed aluminum target

Table 2 Tensile property of the two types of synthesized scaffold and their comparison with a normal nerve tissue [21]

	Normal nerve	Extracted scaffold (random)	Extracted scaffold (aligned)
Ultimate stress (MPa)	6.78 ± 0.57	0.6 ± 0.1	5.2 ± 0.6
Ultimate strain (−)	0.61 ± 0.02	1.14 ± 0.03	1.021 ± 0.002

Considering the results of MTT assay and chromatography technique together, it is presumed that samples of the second group are the best alternatives compared to the other samples.

In the practical aspect of scaffolds' crosslinking, both the aforementioned collagen crosslinking outcomes were probed. As an example, the micrograph of random scaffold which was crosslinked with the aforementioned prior genipin solution (3.5 mM, 5 days) is presented in Fig. 11.

The fraction of attached cells to the scaffold surface was quantitated according to the attachment assay. In Chart 3 the trace of this test can be observed.

4 Discussion

Promoting functional repair after nerve tissue injury is an achievable target. It is likely that the most successful future intervention strategies will involve a combination of approaches, for example, blocking inhibitors of axon regeneration, as well as providing a scaffold for orientated tissue repair. The ideal scaffold to support such axonal regeneration has yet to be developed [22].

The goal of the present investigation is the novel combination of the synthesis of a biodegradable composite scaffold with an oriented fiber structure with genipin as the

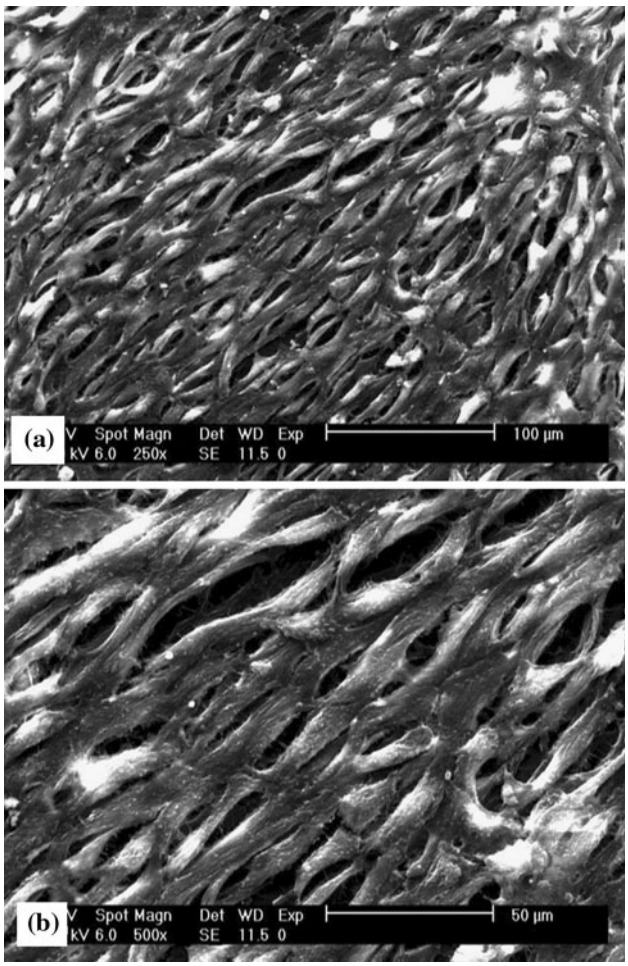

Fig. 8 Cancerous SK-N-MC cell culture on the composite collagen-C6S web with regular aligned fiber structure. **a** ×250 and **b** ×500

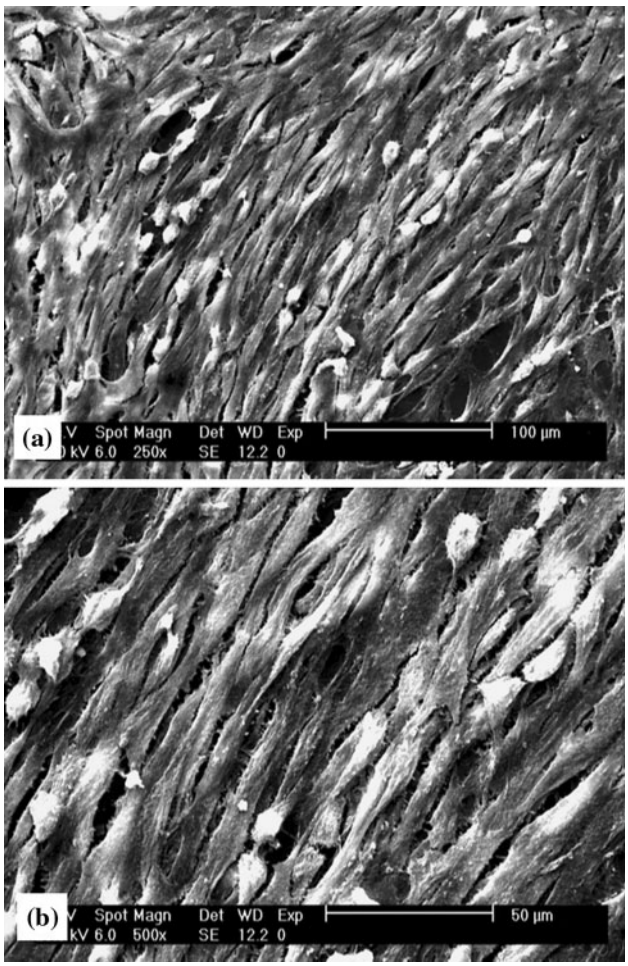

Fig. 9 Normal fibroblast cell culture on the composite collagen-C6S web with regular aligned fiber structure. **a** ×250 and **b** ×500

crosslinking agent. This was accomplished by the method of electrospinning and evaluation of its cytocompatibility.

As the final material composition, Collagen to GAG ratio of 98:2 was chosen. According to the parameters which were optimized during the previous sections, the electrospinning process was run with definite and specified parameters.

Solution viscosity is one of the most influential factors that affect the nanofiber formation. It is directly controlled by the solution concentration. Empirical evidence reported by a number of authors indicates that by increasing the solution concentration, transitions occur from beads to beaded fibers to homogeneous fibers [6].

In polymeric solutions, entanglement of the chains is the determining factor of solution viscosity. As it is discussed in the literatures [7, 23–26], viscosity is a factor in electrospinning process with a minimum threshold value. As long as this value is kept below this threshold, getting the fibrous structure is infeasible. From this point on, increasing the value not only results in fiber formation but also increases the fiber diameter [6]. The higher value of chain entanglement and consequent increase in viscosity, leads to thicker fibers [3, 6].

This may explain the larger mean diameter found in higher concentration solution compared with the other ones as represented in Fig. 2. As our attempt was to attain the nano-sized fibers the concentration of 7% w/v was put as the basis of production.

After viscosity the second most significant factor in electrospinning process is the electric field strength. Electrostatic force is the primary driving force in electrospinning. The jet emerges from the polymer solution as soon as the surface tension of the solution is overcome by this force. Therefore, the applied voltage is important to initiate the jet [6].

According to the researches [27, 28], at lower strengths of the electric field, the dripping of the solution or instability of the jet are the main culprits in bead formation. In Fig. 3a the beaded fibers indicate that the utilized electric field strength can still go higher. At higher strengths, the jet undergoes whipping and uniform fibers are formed as the morphology shown in Fig. 3b. On the other hand, higher

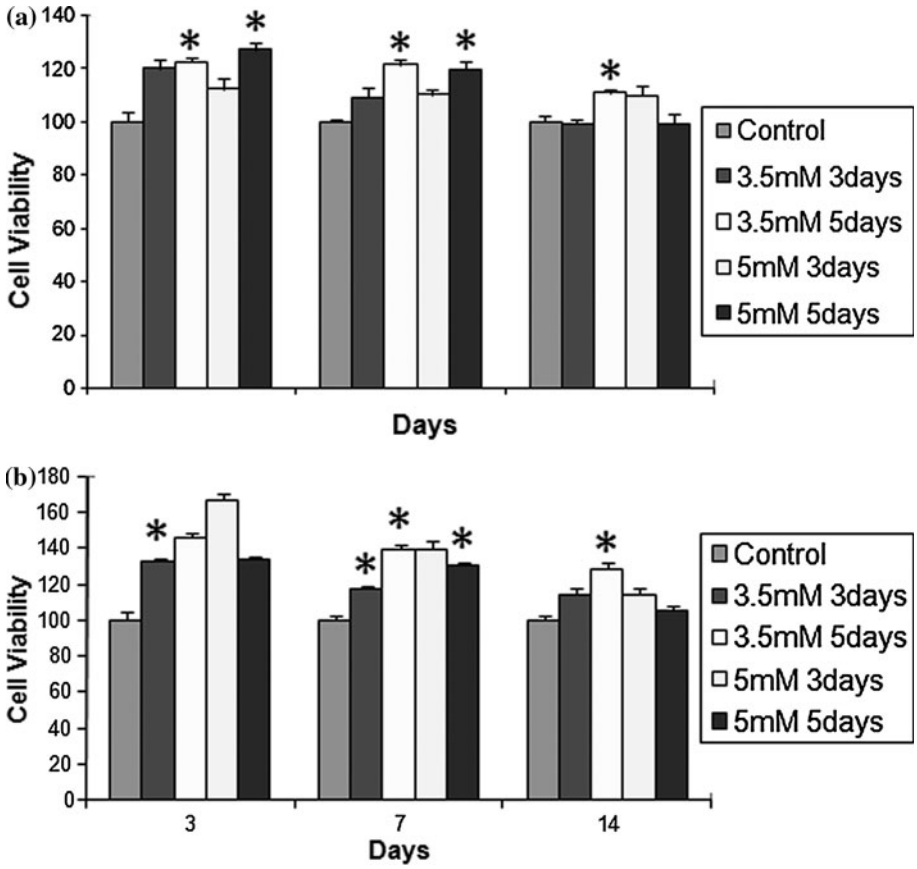

Chart 2 Cell viability versus culturing time (3, 7 and 14 days) of the **a** SK-N-MC cancerous and **b** normal fibroblast cells resulted from MTT assay. Data are expressed as mean ± SD (n = 5). Data were subjected to Dunnet one way analysis of variance (ANOVA), $*P < 0.05$

voltage than that minimally required to obtain bead-free fibers causes bead formation in the fibers [6, 28]. At Fig. 3c the fabricated beaded fibrous structure points to the excessive amount of electric field strength used. This result is attributed to the instability in the initial part of the jet, which correlates with the beaded morphology in the fibers [6, 28]. Consequently, the final electric field strength was set at 15 kV.

Applied voltage and feeding rate are highly interdependent. In order to form uniform fibers, the rate of solution removal from the needle by the electrostatic force has to match with that of the solution mass delivery. Therefore, specific combination of these two parameters can lead to the mass balance.

For a given strength of the electric field, higher flow rate results in the formation of larger diameter fibers with beaded morphologies, and at lower flow rates, mainly dripping of the solution will occur. Accordingly, there exist combinations of these two parameters at which the mass balance can be achieved. However, these combinations highly depend on the type of polymer and solvent used [6].

Considering the aforementioned relationship and the voltage which was set in the previous section, the best results for this type of electrospinning solution were achieved when the solution flow rate and electric field strength were adjusted to 0.2 ml/h and 15 kV respectively. Figure 4 shows how the increases in the solution flow rate, when higher than the minimum rate required, makes the structure more defective.

Nozzle to target distance is among the secondary parameters which affect the web structure. Increasing the distance in the limited range has no definite effect on the mean diameter of the fibers, but affects the homogeneity of the structure. It is concluded that an increase of the distance provides longer time for evaporation of the solvent, and also encourages the extent of the spiraling motion during whipping, consequently, determining a more homogenous structure [6, 28–31]. In Fig. 5 the improving procedure in homogeneity of the mat structure resulted from the increase in amount of nozzle to target distance is presented.

Although in some studies reported in the literature it was concluded that increasing nozzle to target distance results in a reduction in mean fiber diameter [19], according to our findings we concluded that distance is a factor which affects the web structure in two manners: at lower distance range, increasing the distance reduces fiber diameter, and at the higher distance range this phenomenon ceases and influences the structure homogeneity.

In the second main phase of this project an attempt was made to produce an aligned fibrous structure.

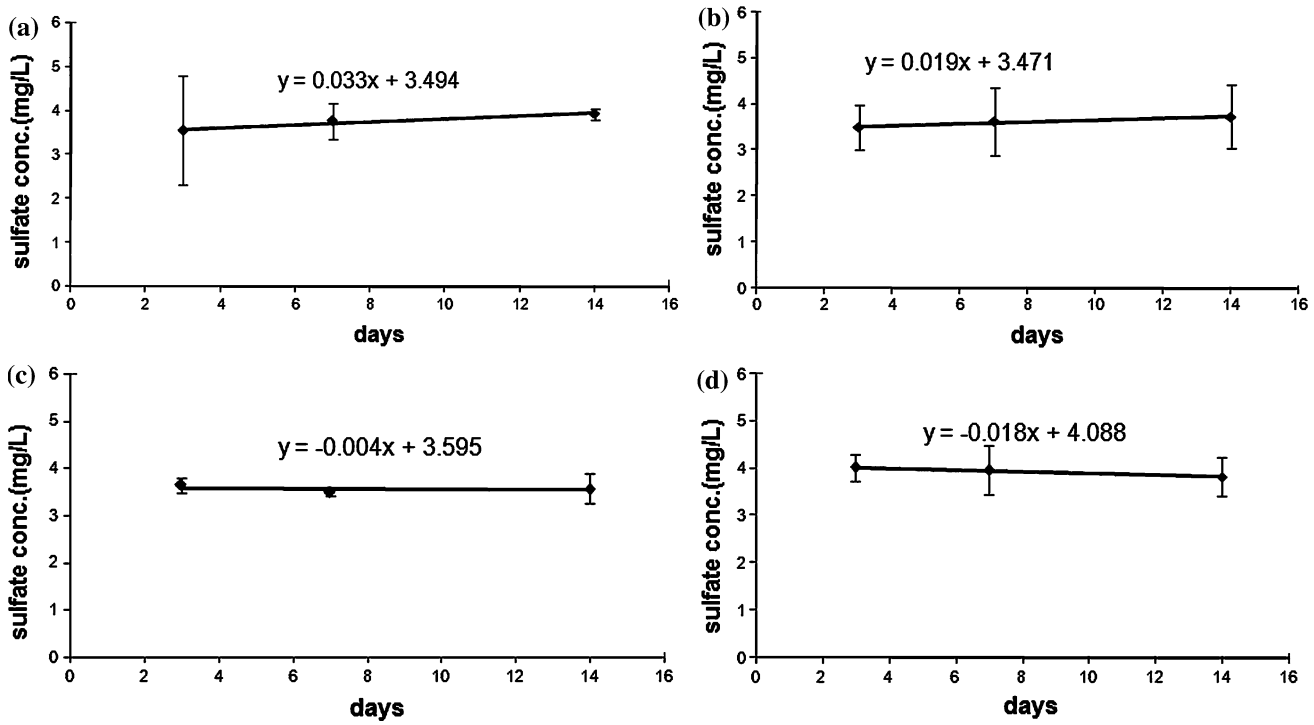

Fig. 10 Release of sulfate factor (proportional to C6S concentration) in the culture medium was defined by Ion Chromatography test. Although the slope of trendlines in all 4 curves (**a** 3.5 mM 3 days, **b** 3.5 mM 5 days, **c** 5 mM 3 days, **d** 5 mM 5 days) is almost zero but since in the curves **a** and **b**, sulfate concentration (mg/l) has an ascendant flow, so the status is more suitable for cell outgrowth. Sulfate concentration ± SD (n = 3)

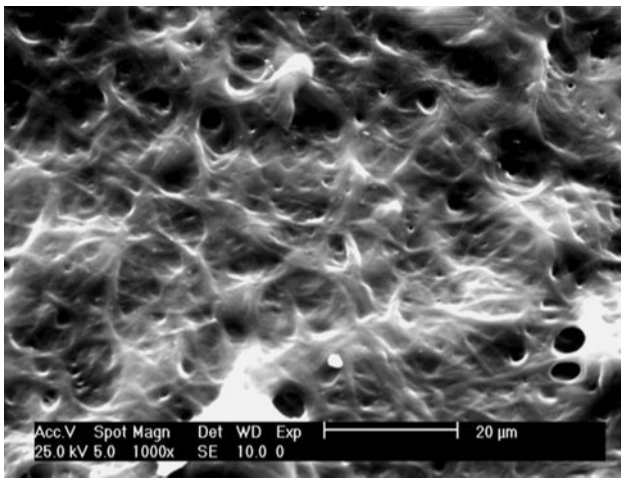

Fig. 11 The cross linked structure of the scaffold with genipin (Mag. ×1,000)

Since the basement characteristics and its structural organization has a profound effect on cell outgrowth organization, and also to improve the mechanical property of the random scaffolds, we strove to get much closer to the structural characteristic of the native ECM.

To achieve the goal, a rotational collector with three adjustable speeds was utilized. Although a perfect regularly aligned fibrous structure was not achieved, the in vitro cell culturing experiment confirmed the affected cell outgrowth organization (Figs. 8, 9).

As cell orientation defines cell function, the electrospinning of a well-defined structure of the scaffold can be very useful for engineering different specific tissues or organs [2, 4].

To increase the biostability property of the mats, they were crosslinked via four distinctive crosslinking solutions. In order to determine the most cytocompatible crosslinking solution among the four, the MTT assay was conducted.

Moreover, the discussion of the MTT assay charts represents a general descending flow of the cell viability factor as time passes. Certainly, one of the influential factors in this form of flow is the release of crosslinking agent. This is the degradation of the mat that causes the release of reacted genipin (the molecules which were embedded in crosslinked structure and are now released) into the medium [16].

Also in this study the release rate of C6S was followed through ion chromatography assay. As mentioned earlier GAGs found to enhance biological interactions with cells and motivate tissue regeneration [2–4]. Accordingly, the ejection of this medium, from the mat into the regenerating environment, would be an inspiring factor. According to the diagrams demonstrated in Fig. 10, the first and the second groups have an ascending release while the third and fourth groups have a descending release profile.

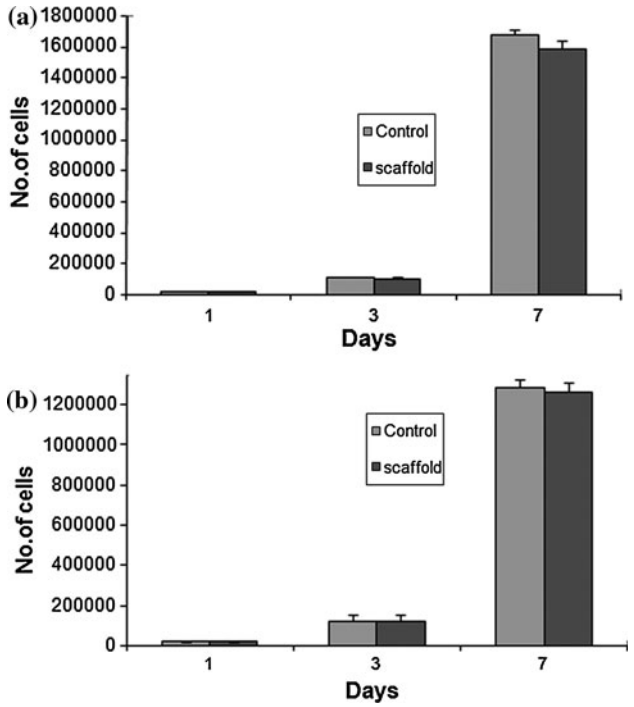

Chart 3 Cells interaction affinity to scaffolds was traced in number of attached cells to scaffold versus culturing time. As far as it is shown in **a** SK-N-MC and **b** fibroblast, there is no specific difference in attachment affinity of cells to scaffold regarding to control sample (*plate bottom*). Number of cells ± SD (n = 3)

It is supposed that, between the concentrations of 3.5 and 5 mM there exists a transition point at which different amount of shrinkage results for scaffolds during crosslinking.

At higher concentrations than the mentioned point, like the third and the fourth group (Fig. 10c, d), the structural shrinkage caused by the crosslinking process inhibits the diffusion of the C6S. The more this value, the more the inhibition of diffusion would be. But, at lower concentration than the mentioned value there would be less shrinkage. Therefore, diffusion of the C6S would be much more convenient.

Based on the C6S release profile and the MTT assay results it is concluded that the applied synhesis factors in the second group is reliable for further and future studies.

According to this study, the application of the novel combination of oriented fibrous collagen/GAG scaffold with genipin crosslinking agent could provide progress in developing in tissue engineering scaffolds.

5 Conclusion

With the aid of nanotechnology, the present study explored the possibilities of fabrication of Collagen-C6S composite nano-structured porous scaffold by electrospinning method. The structure of Collagen-C6S scaffold resembles that of natural ECM in our body in forms of nano-scale fiber diameters ranging between 50 and 350 nm. The average fiber diameter of the scaffold decreased by decreasing the Electrospinning solution viscosity and by decreasing solution flow rate, this was while the electric field strength and the nozzle to target distance were set in their optimum values. With the viewpoint of cells motivation to grow in an oriented path, the electrospun fibers were collected in an organized, aligned manner with the aid of a rotating collector. This was while the in vitro cell culture studies proved the effect of fiber orientation on the corresponding cell growth preference. The statistical data gained from attachment test also indicated the sufficient cell affinity to attach to the surface of the scaffolds. In order to increase the biocompatibility of the scaffolds, they were crosslinked with genipin, within four definite groups of "crosslinking solution concentration, time" combination. The in vitro cell culture studies show the biocompatibility of the scaffold. Additionally, it was the MTT assay results that define the proper group of crosslinking among the four. On the other hand, the close physical and mechanical properties of the scaffold to normal nerve tissue that ensures the successful regeneration of tissue in the scaffold. These findings provide the feasibility of using nano-structured scaffold in nerve tissue engineering for better cell adhesion and outgrowth in vitro. Hence, we propose the application of this method in the future in vivo.

References

1. Langer R, Vacanti JP. Tissue engineering. Science. 1993;260:920–6.
2. Shaoping Z, Wee ET, Xiao Z, Beuerman RW, Seeram R, Lin Yue LY. An aligned nanofibrous collagen scaffold by electrospinning and its effects on in vitro fibroblast culture. J Biomed Mater Res A. 2006;79(3):456–63.
3. Shaoping Z, Wee ET, Xiao Z, Roger B, Seeram R, Lin Yue LY. Formation of collagen–glycosaminoglycan blended nanofibrous scaffolds and their biological properties. Biomacromolecules. 2005;6:2998–3004.
4. Shaoping Z, Wee ET, Xiao Z, Roger B, Seeram R, Lin Yue LY. Development of a novel collagen–GAG nanofibrous scaffold via electrospinning. Mater Sci Eng. 2007;27(C):262–6.
5. Fratzl P. Collagen: structure and mechanics. New York: Springer; 2008.
6. Moghe AK. Core-sheath differentially biodegradable nanofiber structures for tissue engineering. A Dissertation submitted to the Graduate Faculty of North Carolina State University, Raleigh; 2008.
7. Boland ED, Coleman BD, Barnes CP, Simpson DG, Wnek GE, Bowlin GL. Electrospinning polydioxanone for biomedical applications. Acta Biomater. 2005;1:115–23.
8. Dalby MJ, Riehle MO, Sutherland DS, Agheli H, Curtis ASG. Fibroblast response to a controlled nanoenvironment produced by colloidal lithography. J Biomed Mater Res. 2004;69(A):314–22.

9. Vance RJ, Miller DC, Thapa A, Habersroth KM, Webster TJ. Decreased fibroblast cell density on chemically degraded polylactic-co-glycolic acid, polyurethane and polycaprolactone. Biomaterials. 2004;25:2095–103.
10. Mei-Chin C, Hsiang-Fa L, Ya-Ling C, Yen C, Hao-Ji W, Hsing-Wen S. A novel drug-eluting stent spray-coated with multi-layers of collagen and sirolimus. J Control Release. 2005;108:178–89.
11. Bai-Shuan L, Chun-Hsu Y, Shan-Hui H. A novel use of genipin-fixed gelatin as extracellular matrix for peripheral nerve regeneration. J Biomater Appl. 2004;19:21–34.
12. Yueh-Sheng C, Ju-Ying C, Chun-Yuan C, Fuu-Jen T, Chun-Hsu Y, Bai-Shuan L. An in vivo evaluation of a biodegradable genipin-cross-linked gelatin peripheral nerve guide conduit material. Biomaterials. 2005;26:3911–8.
13. Sung H-W, Liang H-C. Acellular biological material chemically treated with genipin. United States Patent 6,545,042, 2003.
14. Gee AO, Baker BM, Mauck RL. Mechanics and cytocompatibily of genipin crosslinked type I collagen nanofibrous scaffolds. Summer Bioengineering Conference (SBC2008), 25–29 Jun, Marriott Resort, Marco Island, USA.
15. Lien S-M, Li W-T, Huang T-J. Genipin-crosslinked gelatin scaffolds for articular cartilage tissue engineering with a novel crosslinking method. Mater Sci Eng. 2008;28(C):36–43.
16. Sundararaghavan HG, Monteiro GA, Lapin NA, Chabal YJ, Miksan JR, Shreiber DI. Genipin-induced changes in collagen gels: correlation of mechanical properties to fluorescence. J Biomed Mater Res A. 2008;87(2):308–20.
17. Sundararaghavan HG, Monteiro GA, Firestein BL, Shreiber DI. Neurite growth in 3D collagen gels with gradients of mechanical properties. Biotechnol Bioeng. 2009;102:632–43.
18. Jose MV, Thomas V, Dean DR, Nyairo E. Fabrication and characterization of aligned nanofibrous PLGA/collagen blends as bone tissue scaffolds. Polymer. 2009;50:3778–85.
19. Baker SC, Atkin N, Gunning PA, Granville N, Wilson K, Wilson D, Southgate J. Characterisation of electrospun polystyrene scaffolds for three-dimensional in vitro biological studies. Biomaterials. 2006;27:3136–46.
20. Adams JC. Methods in cell biology: methods in cell–matrix adhesion. San Diego: Elsevier Science; 2002.
21. Dumont CE, Walter B. Stimulation of neurite outgrowth in a human nerve scaffold designed for peripheral nerve reconstruction. J Biomed Mater Res B. 2005;37B(1):194–202.
22. Mollers S, Heschel I, Olde Damink L, Schugner F, Deumens R, Muller B, Bozkurt A, Gerardo Nava J, Noth J, Brook G. Cytocompatibility of a novel, longitudinally microstructured collagen scaffold intended for nerve tissue repair. Tissue Eng A. 2009;15:461–72.
23. Kenawy E, Layman J, Watkins J, Bowlin G, Matthews J, Simpson D, Wnek G. Electrospinning of poly(ethylene-co-vinyl alcohol) fibers. Biomaterials. 2003;24:907–13.
24. Shenoy S, Bates W, Frisch H, Wnek G. Role of chain entanglements on fiber formation during electrospinning of polymer solutions: good solvent, non-specific polymer polymer interaction limit. Polymer. 2005;46:3372–84.
25. Koski A, Tim K, Shivkumar S. Effect of molecular weight on fibrous PVA produced by electrospinning. Mater Lett. 2004;58:493–7.
26. Jarusuwannapoom T, Hongrojjanawiwat W, Jitjaicham S, Wannatong L, Nithitanakul M, Pattamaprom C, Koombhongse P, Rangkupan R, Supaphol P. Effect of solvents on electro-spinnability of polystyrene solutions and morphological appearance of resulting electrospun polystyrene fibers. Eur Polym J. 2005;41:409–21.
27. Shin Y, Hohman M, Brenner M, Rutledge G. Electrospinning: a whipping fluid jet generates submicron polymer fibers. Appl Phys Lett. 2001;78:1149–51.
28. Deitzel J, Kleinmeyer J, Harris D, Beck Tan N. The effect of processing variables on the morphology of elecrospun nanofibers and textiles. Polymer. 2001;42:261–72.
29. Yarin A, Koombhongse S, Reneker D. Bending instability in electrospinning of nanofibers. J Appl Phys. 2001;89:3018–26.
30. Hohman M, Shin Y, Rutledge G, Brenner M. Electrospinning, electrically forced jets. II. Applications. Phys Fluids. 2001;13:2221–36.
31. Reneker D, Yarin A, Fong H, Koombhongse S. Bending instability of electrically charged liquid jets of polymer solutions in electrospinning. J Appl Phys. 2000;87:4531–47.